eTransportation 20 (2024) 100329

Contents lists available at ScienceDirect

eTransportation

journal homepage: www.journals.elsevier.com/etransportation

Decoding range variability in electric vehicles: Unravelling the influence of cell-to-cell parameter variation and pack configuration

Sourabh Singh [a], Sarbani Mandal [a], Sai Krishna Mulpuri [a], Bikash Sah [b,*], Praveen Kumar [a]

[a] Departments of Electronics and Electrical Engineering, Indian Institute of Technology Guwahati, Guwahati, 781039, Assam, India
[b] Department of Electrical Engineering, Mechanical Engineering and Technical Journalism, Hochschule Bonn-Rhein-Sieg, Sankt Augustin, 53757, North Rhine-Westphalia, Germany

ARTICLE INFO

Keywords:
Electric vehicles
Range variability
Battery pack configurations
Cell-to-cell parameter variations

ABSTRACT

This study addresses the common occurrence of cell-to-cell variations arising from manufacturing tolerances and their implications during battery production. The focus is on assessing the impact of these inherent differences in cells and exploring diverse cell and module connection methods on battery pack performance and their subsequent influence on the driving range of electric vehicles (EVs). The analysis spans three battery pack sizes, encompassing various constant discharge rates and nine distinct drive cycles representative of driving behaviours across different regions of India. Two interconnection topologies, categorised as "string" and "cross", are examined. The findings reveal that cross-connected packs exhibit reduced energy output compared to string-connected configurations, which is reflected in the driving range outcomes observed during drive cycle simulations. Additionally, the study investigates the effects of standard deviation in cell parameters, concluding that an increased standard deviation (SD) leads to decreased energy output from the packs. Notably, string-connected packs demonstrate superior performance in terms of extractable energy under such conditions.

1. Introduction

1.1. Context and motivation

The global shift to EVs has gained momentum rapidly. Reports show a 53% year-on-year (YoY) increase in passenger EV sales during the fourth quarter of 2022, culminating in over 10.2 million units for the year [1]. For instance, India's thriving EV market experienced an impressive 200% YoY growth, exceeding one million units in 2022 [2]. As the EV market grows, range variability has become an important area of research, with considerable implications for electric vehicle performance, usability, and overall market adoption. Lawsuits against original equipment manufacturers (OEMs) have emerged due to discrepancies between claimed and achieved ranges, further emphasising the need to study range variability in EVs [3]. Although internal combustion engine vehicles (ICEs) also display range variability, the factors influencing EVs are far more complex and multifaceted, including driving applications, intensities, and patterns [4].

Surprisingly, even two identical make and model EVs can show up to 6.88% range variability under the same driving conditions (refer to Section 3.1). This intriguing phenomenon raises a critical question: Can the underlying causes of this variability be discovered, and can they be mitigated during the pack design process?

1.2. Literature review

Studies have identified the differences between cells of the same chemistry from the same manufacturer as the main cause of this variability [5]. This difference is investigated in this study by considering the variations in two key independent cell parameters, which are the nominal voltage and the rated capacity, as shown in Fig. 1.

Dubarry et al. explored the subtleties of cell-to-cell variation [7], laying the foundation for a deeper understanding of the issue. However, these findings also raise further questions about optimising battery pack performance and reducing variability. Table 1 offers a comprehensive overview of the research conducted by various groups in this rapidly evolving field. Despite the wealth of knowledge accumulated on this topic, a definitive answer to these questions remains elusive.

The studies in the literature reviewed revealed three major directions of research in the context of analysing cell-to-cell variations: (i) methods to analyse cell-to-cell variations and the different ways the cells can be connected, (ii) influence of cell-to-cell variations on the overall energy delivered by the battery pack, and (iii) studying the impact of different cell connections on the battery pack's energy delivery. The analysis of cell-to-cell variations and the different ways

* Corresponding author.
E-mail addresses: sourabh.singh@iitg.ac.in (S. Singh), sarbani.mandal@iitg.ac.in (S. Mandal), m.sai@iitg.ac.in (S.K. Mulpuri), bikash.sah@h-brs.de (B. Sah), praveen_kumar@iitg.ac.in (P. Kumar).

https://doi.org/10.1016/j.etran.2024.100329
Received 7 July 2023; Received in revised form 29 February 2024; Accepted 1 April 2024
Available online 3 April 2024

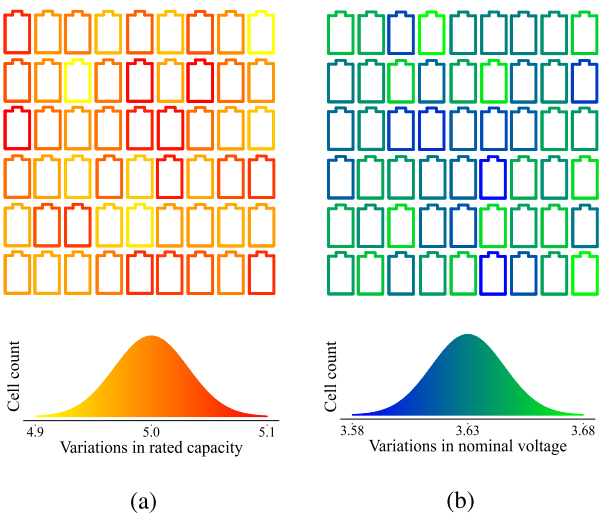

Fig. 1. The figure illustrates the (a) rated capacity and (b) nominal voltage variations of cells within a battery pack, assumed to conform to a normal distribution. The normal distributions in cell parameter variations were derived from the standard deviations obtained from the work of Xie et al. [6]. The cells are randomly distributed throughout the pack, mimicking the pack manufacturing process.

Table 1
Literature review of the studies involving the effects of cell-to-cell variations on pack energy output.; CE refers to the study of pack capacity estimation; VC refers to the consideration of cell parameter variations; CX refers to different cell connections considered while making the pack; OV refers to differences in output energy of pack studied for cell variations, RV refers to variations in EV driving ranges studied, and LP refers to sufficiently large pack taken for study (at least 25 cells).

Reference	CE	VC	CX	OV	RV	LP
[5]	No	Yes	No	No	Yes	Yes
[6]	No	Yes	No	No	No	No
[7]	No	Yes	No	No	No	No
[8]	Yes	Yes	No	Yes	No	No
[9]	No	Yes	No	No	No	No
[10]	No	Yes	No	No	No	Yes
[11]	Yes	Yes	No	Yes	No	Yes
[12]	Yes	Yes	No	No	No	Yes
[13]	Yes	No	No	No	No	No
[14]	No	Yes	No	No	No	No
[15]	Yes	Yes	Yes	Yes	No	No
[16]	No	Yes	No	Yes	No	Yes
[17]	No	Yes	Yes	No	No	Yes
[18]	No	Yes	No	No	No	No
[19]	No	Yes	No	No	No	Yes
[20]	Yes	Yes	Yes	Yes	No	No
[21]	No	No	No	No	Yes	No
[22]	No	Yes	No	No	No	No
[23]	No	Yes	No	No	No	No
[24]	No	Yes	Yes	No	No	No
[25]	No	Yes	Yes	No	No	No
[26]	No	Yes	No	No	No	No
[27]	No	Yes	No	No	No	No
[28]	No	Yes	No	No	No	No
[29]	No	Yes	No	No	No	No
[30]	No	Yes	No	No	No	No
[31]	No	Yes	Yes	No	No	Yes
[32]	No	Yes	No	No	No	No
[33]	No	Yes	No	No	No	No
[34]	No	Yes	No	No	No	No
[35]	No	Yes	No	No	No	No

the cells can be connected was the focus of [17,24,25,31]. Dubarry et al. [17] examined a sizable cluster comprising 49 cells, investigating both individual cell responses and their collective behaviour within a battery pack. The study delved into pack performance across configurations of 1s49p, 49s1p, and 7s7p while exploring variations in cell SoC, SoH, and capacity. They concluded that the performance can be additive when cells are connected in series. However, in cases where cells are connected in parallel, variations between individual cells exhibited minimal impact on the overall battery pack performance, largely due to the possibility of self-balancing. Rumpf et al. [24] employed a comprehensive model for lithium-ion cells to analyse the current distribution within various cell connections in a module. On the other hand, Song et al. [25] utilised a primitive electrical model to study cell-to-cell variations over time under different cooling structures and considered the influence of cell connections. Ganesan et al. [31] explored capacity fading in different modules over hundreds of cycles.

The influence of cell-to-cell variations on the overall energy delivered by the battery pack was a focal point in the studies by [8,11,16]. Liu et al. investigated current distributions over time in a group of cells connected in parallel, emphasising the impact of placing higher impedance cells in parallel on the total output energy [8]. An et al. proposed battery pack inconsistency models and evaluated how variations in model parameters affect the pack's output energy [11]. Zhou et al. [16] identified Coulomb efficiency, temperature difference, and capacity fading as the primary factors affecting the pack's consistency.

In addition to examining cell-to-cell variations, [15,20] also studied the impact of different cell connections on the battery pack's energy delivery. Miyatake et al. [15] analysed 12 real cells with slightly different characteristics and demonstrated that fewer cells in series delivered higher discharge capacity (Ah). Luan et al. [20] considered various connection topologies and found that cross-connections delivered the most energy. However, it is worth noting that the pack size considered in these studies was relatively small, and their analysis lacked range analysis on EVs.

Chen et al. conducted pioneering research on the effects of cell-to-cell variations on the range of EVs while accounting for cell-to-cell parameter variations [5]. They simulated an EV with a large battery pack operating on a specific drive cycle. However, their approach of randomly choosing standard deviations in parameters led to a disconnect between simulation data and real-world outcomes. Additionally, Chen et al. did not explore the impact of different pack configurations on EV range.

Numerous other research [6,7,9,10,14,18,19,22,23,26–30,32–35], directed their efforts towards investigating cell-to-cell variations and deriving insights concerning variations in parameters such as impedance, cycle life, capacity, and voltage. The conclusions and methodologies drawn from their studies greatly contributed to developing an understanding and shaping the approach employed in this current work. Several of these references will be cited subsequently in the following sections.

Overall, the literature review has shed light on the study of cell-to-cell variations. However, a concrete answer to the question of range variability requires consideration of appropriate parameters.

One common limitation observed in most of the reviewed literature is the consideration of battery pack sizes that are not large enough to mimic real-world EV packs. These smaller pack sizes result in a limited number of discharge paths, which may not accurately reflect the behaviour of larger packs with numerous cells interconnected in series and parallel. Moreover, cell parameter variations can significantly affect the current distribution, leading to imbalances in the current delivered by parallelly connected cells.

Experimental validation of multiple battery packs with different cell-to-cell connections is another major challenge due to resource constraints, such as the number of cells and the time required for charging and discharging the packs.

In contrast to using basic electrical models for Li-ion batteries, the battery model employed in this work was calibrated with data from PyBaMM, which will be further elaborated in the Experimental Validation section. This calibrated model offers the potential for more accurate and reliable results in understanding the impact of cell parameter variations on EV range.

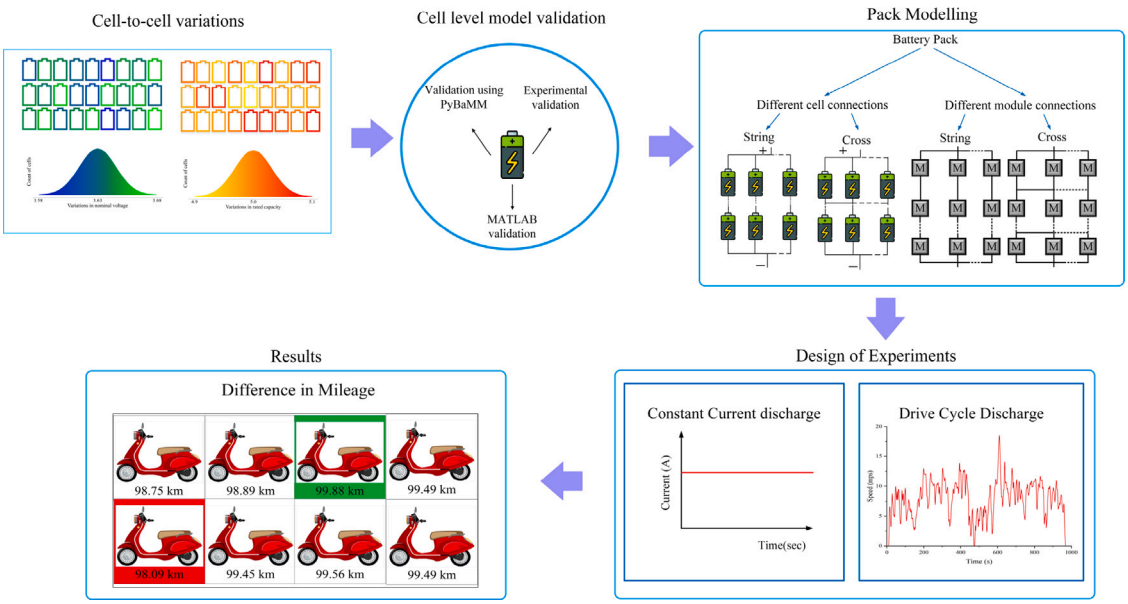

Fig. 2. Summary of the research presented in the manuscript.

The core concept driving this research is encapsulated in the diagram presented in Fig. 2. Fundamentally, the study is built upon the foundations of studying the effects of cell-to-cell variations in nominal voltage and rated capacity. To enact this, a cell model is employed, which is validated with the PyBaMM model available based on experimental characterisation already published in the literature. Further, experiments in the laboratory are also performed on an LG M50 cell to validate the calibrated model. Using the cell modelled, multiple packs are prepared in which the cell-to-cell variations studies are performed, each characterised by distinct cell-to-cell and module-to-module connections. Through comprehensive examination across varying C rates and drive cycles, this approach sheds light on the spectrum of range variability observed in electric vehicles (EVs).

1.3. Contributions of this work

Based on the challenges and drawbacks determined in the literature, this study aims to unravel the complexities of range variability by examining the contributing factors and proposing innovative strategies to mitigate the differences in the extractable output from a battery pack during design and manufacturing. The following are the major contributions:

- A methodology to analyse the impact on extractable energy and driving range due to the cell parameter deviation, cell connections, battery configuration, battery pack size, and driving behaviour. The methodology is the workflow followed in the analysis performed in this work.
- An empirical model is proposed that accurately predicts the extractable energy from a fresh battery pack and quantifies the deviation in extractable energy for different packs of the same configuration, enabling effective design and manufacturing strategies and performance optimisation.
- 74 possible battery pack configurations were studied based on the methodology proposed in the work under constant charge–discharge and real-world driving conditions. The study determines the differences in the vehicles' driving range, which further helps to decide the suitable configuration and cell-to-cell connections for maximum extractable energy.

Further, to replicate all the work presented in the article in experiments, we calculated that at least a minimum of 1.1 million cells, which amounts to about 20 MWh of capacity, will need to be bought, measured and binned according to the standard deviation in their cell parameters, 27 568 unique packs would have to be made. Additionally, all the battery management systems and measurement electronics costs, the charging and discharging of all the packs, and then finally, reading all the data would need to be accounted for. This feat would be impossible for a research group to complete. There are two options for performing the work (i) using data based on models in which either field or synthetically generated data is used and (ii) developing a simulation model calibrated experimentally.

Acquiring field-tested data that accurately reflects real-world battery operation remains difficult [36]. However, within the realm of synthetic data generation, various models [37–40] have made significant contributions, with a common technique being the revolutionary Generative Adversarial Network (GAN) proposed by Ian Goodfellow [41]. Although highly accurate, GAN models have often encountered challenges like model collapse [42,43], instability [44], and convergence evaluation [45], which question their reliability. Hence, simulations using experimentally evaluated models are one of the practical ways to analyse the pack behaviour at such a scale. Although the results presented in this article are based on simulation, the battery cell models are calibrated with the experimental data already published in the literature. Further, with the experimental calibration of the cell model performed in the laboratory, we have ensured that our synthetic data is reliable. More details of the calibration are presented in the Methods section. Our research contributes to the ongoing pursuit of minimising pack-to-pack variability and extending battery pack lifespan, marking a significant step forward in the search for sustainable transportation solutions.

1.4. Article organisation

The remaining sections of the article are organised as follows: Section 2 presents the methodology followed and discusses about the different pack layouts considered, cell model validation, and the design of experiments. Section 3 presents the results based on the methodology proposed for constant discharge and drive cycle-based discharge scenarios. Section 4 presents an empirical model derived from the results of all the simulations. Section 5 discusses the assumptions and limitations considered. Section 6 is the discussion of all of the observations made from the results. Finally, Section 7 concludes the research by summarising the research.

Table 2
Illustration of all the pack sizes, some of the modules used and the abbreviations used for different configurations.

(a) Specifications of three types of packs included in this analysis.

Pack rated capacity (kWh)	Pack rated voltage (V)	Pack size
2.5	48	14s9p
5	48	14s18p
10	72	21s24p

(b) Some of the cell and module connections used

Cell-to-cell connection		Module-to-module connection		Pack size
Type	String/Cross	Type	String/Cross	
14s1p	String	1s9p	String	14s9p
7s3p	String	2s3p	Cross	14s9p
14s3p	Cross	1s6p	String	14s18p
7s6p	Cross	2s3p	Cross	14s18p
21s3p	Cross	1s8p	String	21s24p
7s6p	String	3s4p	Cross	21s24p

(c) Abbreviations used to represent various cell and module connections. The "Inter-module" column refers to the connections of the cells inside the modules, and the "Intra-module" column refers to the connections between the modules, both of which can either be "String" or "Cross". A string connection is represented by a "|" and a cross connection is represented by an "X" in the abbreviations. For example, 7s6p-|X would mean a battery pack that has multiple modules of size 7s6p, with cells inside the module connected in a cross and the modules connected with each other in a string.

Module	Connections		Abbreviation
	Intra module	Inter module	used
7s6p	String	String	7s6p-||
7s6p	Cross	String	7s6p-X|
7s6p	String	Cross	7s6p-|X
7s6p	Cross	Cross	7s6p-XX

2. Methodology

2.1. Experimentation

A series of simulation experiments were conducted to comprehensively investigate the impact of variations in cell parameters on the capacity of battery packs. All possible inter-cell connections were considered to analyse the effect of cell parameter variations on the pack's capacity. Due to the vast number of inter-cell connections and parameters investigated, it was essential to keep the pack size large enough for meaningful analysis while keeping the simulation time within acceptable limits. Different battery pack sizes, including 2 kWh and 5 kWh at 48 V, and 10 kWh at 72 V, were employed to validate the proposed method in relation to pack size. The specifications of the three types of packs are outlined in Table 2a. All the packs were constructed using cell data from LG M50 cells [46], which have a nominal voltage of 3.63 V and a nominal capacity of 18.2 Wh.

To facilitate simulations, all configurations were modelled in Simulink. However, the Simulink cell model's accuracy depends on the proper estimation of parameters, which poses a major challenge. To address this challenge, the cell model's parameters were calibrated with cell discharge data at each C-rate to ensure a computationally fast model with reasonable accuracy. The calibration process is elucidated later in the following subsection of this study, while a flowchart of the process is shown in Fig. 3.

Modules with parallel cells were implemented with two designs: string connections and cross-connections. String connections have cells connected in series, and the only parallel connection is at the module's terminals. Cross-connections have all the connections of a string, but the inter-terminal connections of other cells with similar voltages are also connected. A modular pack design was chosen during battery pack modelling, and packs were made with various modules. Similarly to cells, modules were also connected in a string and cross. Fig. 4 illustrates the various combinations of cell connections. Fig. 4(a) shows a module with m cells connected in series; we are calling this a string, and n such strings of cells connected in parallel. Therefore, the module comprises of $m*n$ cells. Fig. 4(b) is similar to the module in Fig. 4(a), except for the intra-string cross-connections. Similarly, the modules can be connected in string or cross-connections, as shown in Figs. 4(c) and 4(d), respectively. In the figures showing the modules connections, p represents the number of modules in a string connected in parallel, and q denotes the number of such strings connected in series, resulting in a total of $p*q$ modules in a pack.

Table 2b shows a few cell connections, pack sizes, and module size combinations. As the intra-module and the inter-module connections can either be string or cross, represented by "|" or "X" in the abbreviations, there are four possible cases for connections, as illustrated in Table 2c. Similarly, abbreviations for all other modules and connection combinations can be created. Abbreviations for all the different cell connections for different packs can be found in the supplementary.

This study focuses on analysing the variations in pack performance due to cell parameter variations. To accomplish this, multiple packs, specifically 20, need to be made to analyse the differences in packs of identical connection topology. This process is simulated with battery pack models using MATLAB Simulink.

All unique pack connections/topologies have a distinct Simulink model corresponding to them. To analyse the output of 20 packs, the corresponding model of the selected battery pack topology is simulated 20 times. During the initialisation of each simulation, each cell's nominal voltage and rated capacity parameters are generated from a normal or Gaussian distribution. At the same time, all other dependent parameters are calculated from these two parameters by utilising the calibration constants. Therefore, the output of these twenty simulations is equivalent to the output of twenty different packs made.

2.2. Experimental validation

In our work, we address the critical challenge of assessing the impact of variations in cell parameters on the capacity of battery packs. Conducting extensive experimental investigations involving a multitude of configurations and pack sizes is not only impractical but also resource-intensive and time-consuming. To overcome these limitations, we have employed a comprehensive simulation-based methodology to expedite the validation process. Our simulations involve a substantial number of configurations and pack sizes, with 74 different models to be simulated at different C rates and various drive cycles, which overall comes out to more than 28 120 simulations.

2.2.1. Experiments behind PyBaMM data

The parameters related to LGM50 were obtained from a thorough set of experiments conducted by Chen et al. and Nyman et al. These studies extensively characterise the physical, chemical, and electrochemical properties of the LGM50 cell through a diverse array of experimental techniques. Notably, critical parameters pertaining to electrode and cell thermodynamics, kinematics, and transport properties were acquired from electrochemical tests employing a lithium metal reference electrode in a three-electrode configuration [47]. This approach provides insights into individual electrode potentials, cell stoichiometry, and lithium content within the electrodes. Additionally, the open circuit voltage (OCV) of the cells has been determined based on data extracted from galvanostatic intermittent titration technique (GITT) experiments.

The physical properties of cell components, including electrodes, separators, and current collectors, were meticulously obtained through direct measurements following cell disassembly [47]. The parameters which are related to mass transport phenomena within the electrolyte were obtained through a set of electrochemical methods, with ionic

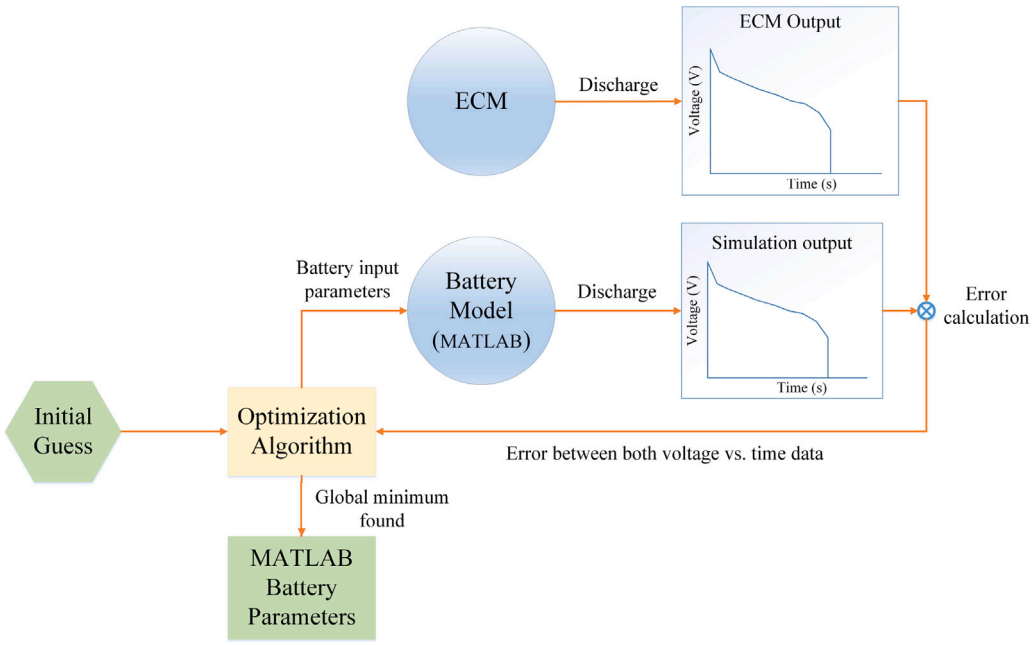

Fig. 3. Calibration process of the battery model with the help of Electro-Chemical Model (ECM) of the LG cell.

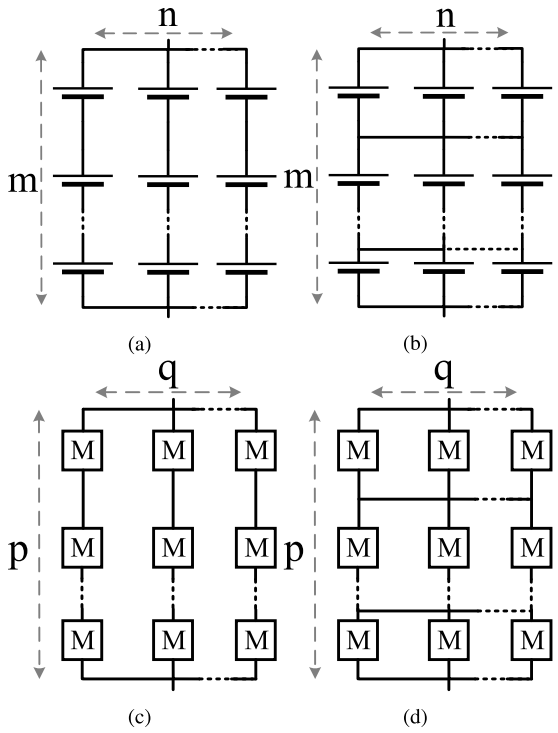

Fig. 4. Description of cell connection names used in this work, i.e. string and cross, here 'M' represents a module. (a) Intra-module string connection of cells. '*m*' cells in series and '*n*' cells in parallel. (b) Intra-module cross-connection of cells. (c) Inter-module string connection. '*p*' modules in series and '*q*' modules in parallel. (d) Inter-module cross connection.

conductivity, diffusivity, and transport number assessed via a standard conductivity meter [48]. Galvanostatic polarisation and concentration cell experiments have provided invaluable insights into diffusion coefficients, and thermodynamic factors of the salt [47]. Our simulation results are backed up by this experimentally verified parameter data, offering a robust and expedited means of conducting capacity-validating experiments while upholding the reliability of outcomes.

2.2.2. Standard life cycle experimentation and calibration

To further strengthen the credibility of our simulation findings, a comprehensive cycle life experiment specified by the manufacturer was conducted on the designated LGM50 cell within our laboratory, spanning approximately 100 h and involving 15 complete cycles. The objective of this attempt was to gauge the concurrence between the simulation outcomes and real-world experimental results. Both Simulink and Pybamm models, to which the Simulink model was calibrated, were subjected to the same manufacturer-prescribed life cycle test. The obtained simulation results were meticulously compared with the life cycle data obtained from the physical experiment to ascertain their degree of agreement.

The practical cycle life assessment involved the development of a specialised environmental cell testing chamber in-house (Fig. 5). The LGM50 cell underwent the standard manufacturer-specified cycle life protocol, which involves distinct charging and discharging stages [46]. During charging, a consistent current rate of 0.3C (1.44 A) was applied until the cell voltage reached 4.1 V, followed by a phase of constant voltage charging at 4.1 V until the current attained 240 mA. A subsequent intermission of 10 min ensued before the cell was subjected to discharge, wherein a constant current rate of 0.5C (2.4 A) was maintained until the voltage reached 2.85 V, followed by a rest period of 20 min. This cycle was diligently replicated over the course of 15 cycles, with the ambient chamber temperature regulated at 25 °C throughout. The terminal voltage profiles for all three scenarios – experimental voltage, Simulink-simulated terminal voltage output, and Pybamm-simulated voltage output – were meticulously analysed. In Fig. 6(a), the combined voltage plots for the final 20 h of operation are showcased for enhanced clarity.

In addition to the comparison of the terminal voltage, differential capacity is another important parameter, which, in the form of graphical representations, serves as a distinct signature for a battery system, permitting continuous monitoring over its lifespan. The differential capacity analysis is a widely utilised approach to evaluate battery health, achieved by pinpointing peaks linked to active material phase transitions. This technique has demonstrated its utility in both diagnosing and predicting battery conditions. Alterations in these plots offer valuable insights into the system's future performance. In this investigation, we analysed the manufacturer-recommended C rates and offered a visual comparison of the outcomes in Fig. 6(b). The

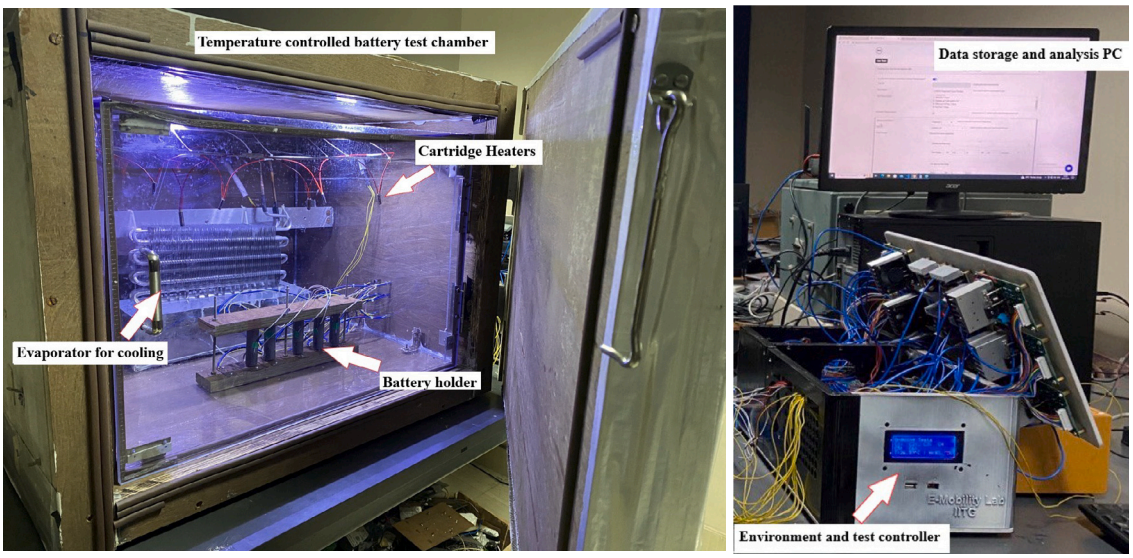

Fig. 5. (a) Temperature controlled, indigenously designed cell testing chamber. The temperature can be increased with the help of cartridge heaters and decreased with the refrigeration unit (Condenser). The battery holder allows for a quick change of cells and can hold up to a maximum of six cells. (b) The controller keeps the temperature constant at a pre-specified level and ensures that the cells are cycled at the desired C-rates or drive cycles. The controller can be programmed with the Data storage and analysis computer.

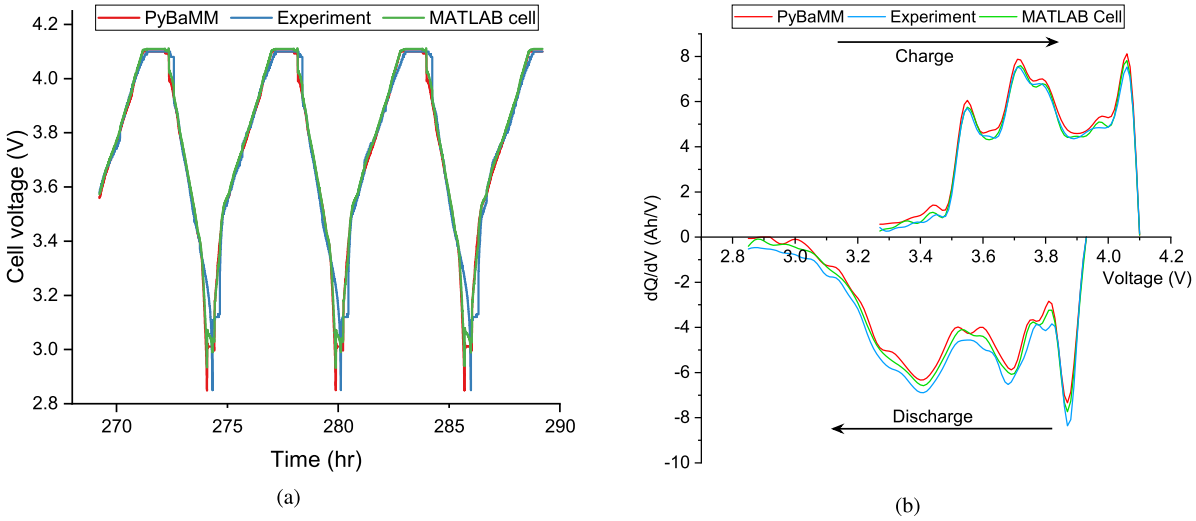

Fig. 6. (a) The final 20 h of the manufacturer-specified cycle protocol for the PyBaMM and MATLAB cell models, along with the experimental result of the LG M50 cell. It should be noted that the MATLAB cell model follows the other two curves closely. (b) Differential capacity analysis has been performed on the manufacturer-specified cycle life experiment, and the obtained results have been compared. The accompanying figure illustrates the degree of alignment between the models and the experiment, thereby affirming the validity and robustness of both the Pybamm and Simulink models.

close correspondence observed among these profiles not only strengthens the confidence in our experimental approach but also validates the robustness of the simulation outcomes obtained throughout our investigation.

2.3. Design of experiments

The experiments were conducted using various pack models designed for the three pack sizes specified in Table 2a. These pack models were classified based on their cell-to-cell and module-to-module connections, as string and cross-connections, as depicted in Fig. 4. In total, a comprehensive set of 74 distinct models was created to investigate the influence of pack topology on pack performance. The cell parameters within these models were subject to variations following normal distributions in nominal voltage and capacity, as previously discussed. Within each of the 74 models, there were 20 instances of cell parameter variations. These instances underwent simulation to discharge at five different C rates and throughout various drive cycles. Moreover, for a specific pack configuration, 14s1p-‖ of the 14s18p pack, a total of 140 instances were generated, each representing 20 instances for 7 increasing standard deviations in cell parameters. These 140 instances were simulated for discharge at five C rates.

The battery pack simulations commence with the generation and calculation of all cell parameters. At the outset, all cells are set to 90% state of charge (SoC). Two types of simulations are conducted for each pack model, one with a constant current discharge rate of packs and the other where they are discharged according to drive cycles.

During the discharge phase, the SoC of each cell in the battery pack is monitored. Once the first cell reaches the lower SoC limit of 10%, the pack discharge is halted to prevent over-discharge damage to any cell. The discharge is then followed by a 1 C constant current charge. Once again, the SoCs of all cells are monitored, and the charge is stopped as

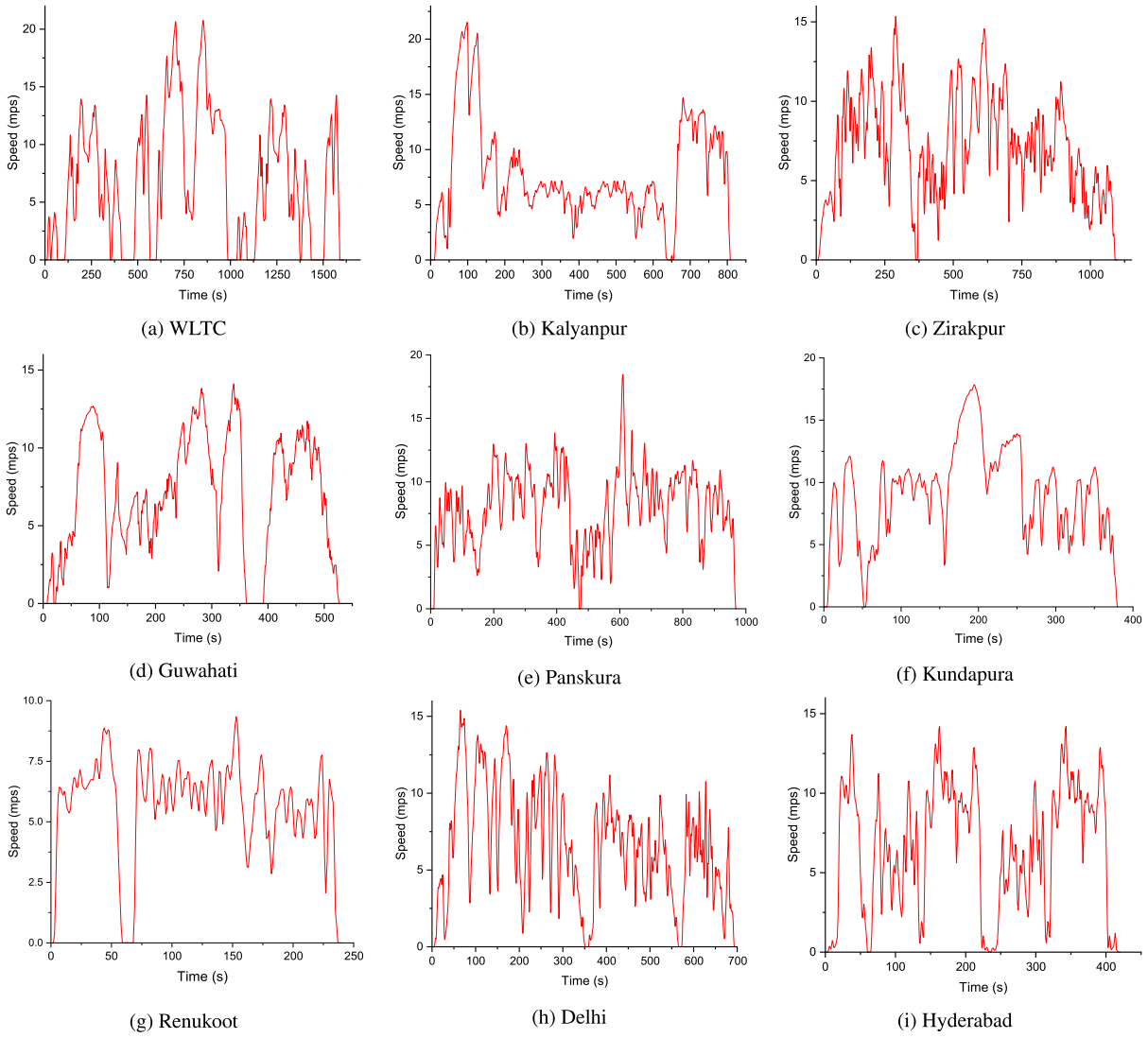

Fig. 7. The figure depicts the nine unique driving patterns employed in this research for evaluating the EV range. While the (a) WLTC follows a standardised drive cycle, the other drive cycles labelled (b) through (i) were derived from our prior research efforts. These diverse drive cycles capture varied driving behaviours across different regions of India, contributing to a comprehensive analysis. The process of creating these specific drive cycles is elaborated upon in [49].

soon as the first cell reaches the maximum SoC limit of 90% to prevent overcharging of any cell. This entire operation constitutes one cycle, and two initial cycles are analysed in this work.

The constant C-rate discharge of the model is carried out at five different C-rates, with a constant interval of 0.5C, ranging from 0.5C up to 2.5C.

For the analysis of the EV range, a total of nine distinct drive cycles were employed. Among these, one was the Worldwide Harmonised Light Vehicles Test Cycle (WLTC), while the remaining eight cycles were derived from prior research conducted by our team. However, to comprehensively study the behaviour of electric two-wheelers in the Indian driving scenario, the remaining eight drive cycles were chosen from different parts of India, depicting different driving conditions. The Indian drive cycles were derived from the previous work conducted by our team [49]. These drive cycles can be seen in Fig. 7. To create these eight additional cycles, eight members of our group rode their two-wheelers across various cities in India, encompassing both urban and rural areas. Each member selected a specific route and undertook three trips at different times of the day, spanning three weeks. This collected data was then utilised to construct unique drive cycles for each location. Incorporating these drive cycles into our study necessitated the transformation of speed-time data into power-time data while considering numerous parameters related to the electric two-wheeler drivetrain. The resulting power-time data was replicated multiple times to ensure that the battery packs reached the termination condition during discharge. A comprehensive account of this entire procedure is documented here [49].

During one of the twenty simulations for a specific pack size model, all the cell parameters are recorded according to the cell distribution. These parameters are then updated in all the remaining models of the same pack size. As a result, the nth cell of each model for a particular pack size will have the same parameters. This approach ensures that the output data for a pack is comparable in every simulation.

The initial step in setting up the pack models for simulations is to calculate the variations in cell parameters for all the cells in the pack based on the previously derived voltage and capacity distribution. As explained earlier, all the pack configurations get identical cell variations. Subsequently, the pack models undergo either constant discharge or discharge following a drive cycle. This proposed methodology is further illustrated in the flowcharts depicted in Fig. 8. To evaluate the performance of vehicles equipped with the battery packs investigated in this work under real-world driving conditions, charge–discharge experiments were conducted for all models across each pack size. The simulations were aimed at determining the duration of the vehicles'

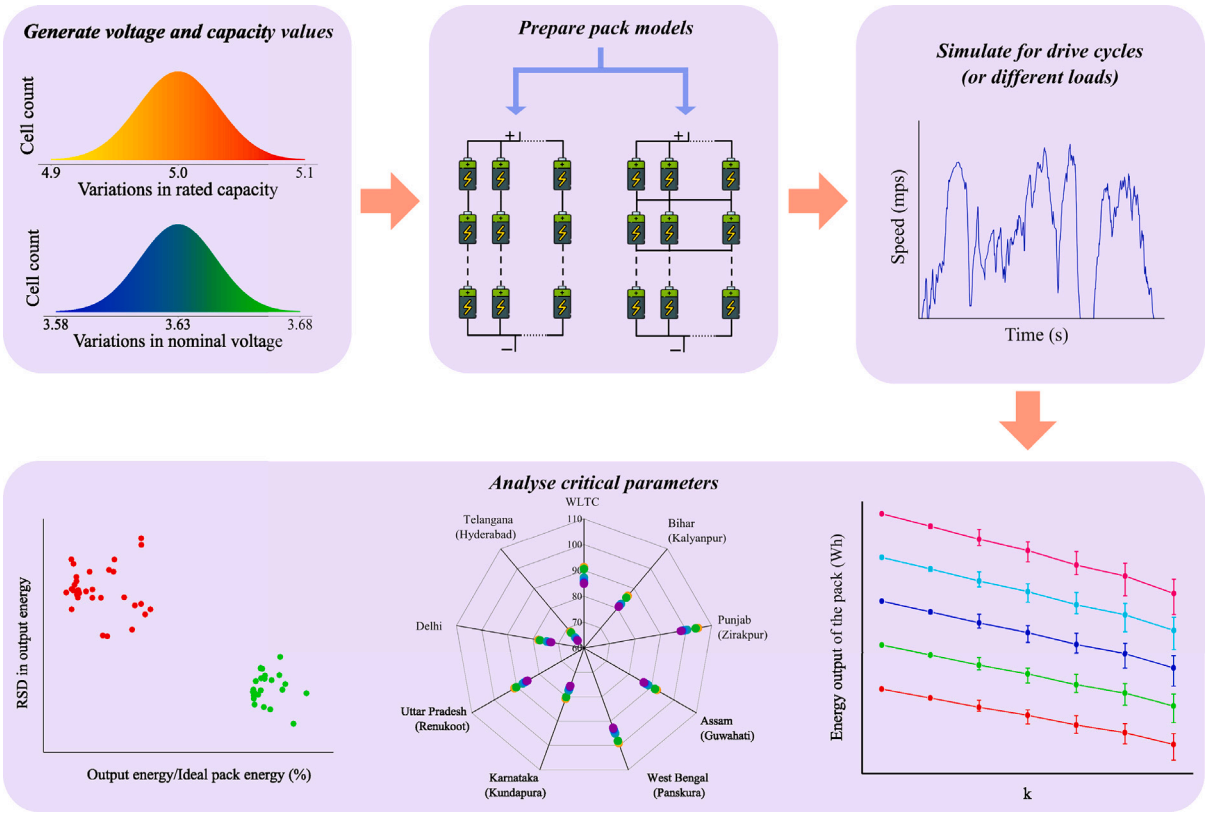

Fig. 8. Pack simulation process.

driving time before the battery pack energy is depleted, reaching the lower SoC limit as described previously. Subsequently, utilising appropriate calculations as discussed in [49], the speed-time data obtained from the drive cycles was transformed into battery power output versus time. This power output drive cycle was repeated until the battery pack energy was exhausted.

3. Results

We employed the battery model of MATLAB Simulink and calibrated the cell parameters with LG M50 cell data [46,47] using PyBaMM, to ensure the accuracy of our findings, as this is a well-understood cell [50]. We investigated battery packs with three distinct energy capacities, which are, 2.5 kWh, 5 kWh, and 10 kWh, as shown in Table 2a, which are the typical pack capacities available in electric two and three-wheelers. A total of 74 battery pack models, with different cell and module connections, are created for these three pack sizes. All these models are briefly described in Table S1 of the supplementary section. Our systematic approach entailed conducting 20 instances of each configuration for 5 constant discharge rates and 9 drive cycles, using an e-2W as the test case. We executed 28,120 simulations and conducted comprehensive statistical analyses to categorise pack configurations and identify the optimal pack based on maximal extractable energy, minimal performance variability, maximum range and the least divergence of cell SoCs.

In this study, 'ideal pack energy' refers to the ideal or the theoretical amount of energy that the battery pack is considered to have. This is the product of the 'Number of cells in the pack' with the 'Energy output of a single cell from fully charged to fully discharged state'. Here the parameters of the cell used are equal to the rated values from the cell datasheet.

3.1. Comparison at constant discharge rate

Our results reveal that the difference between the ideal and delivered pack energy strongly correlates with the standard deviation (SD) in cell parameters. By comparing various pack configurations, we found that cell-to-cell connection patterns significantly affect pack energy output. From our analysis, these patterns can lead to a decrease up to 7.74% in energy, comparing the best and the worst configuration. Drive cycle analyses indicated that distinct pack configurations could produce a 7% difference in driving range between them.

The inferiority of cross-connected configurations can be seen in Fig. 9, where the points for string connections show better energy output and lower SD. Furthermore, as SD in cell parameters double, the decrease in energy output relative to the ideal pack energy approximately doubles as well. Lastly, discharging a battery pack with cells of unequal parameters leads to SoCs of cells diverging during discharge, which is associated with the pack configuration and the SD of cell parameters.

We focus on two pack configurations, 14s1p-‖ and 14s9p-X| for pack 14s18p. The abbreviations used to represent the cell and module connections are explained briefly in Table 2c. The abbreviations of all the models used in this work are available in Table S1 of the supplementary section. We simulated 20 instances of these pack configurations to discharge at five different rates. The energy delivered by the packs is illustrated in Figs. 10(a) and 10(b). It is evident that the variations in cell parameters in each of these 20 instances have impacted their energy output. For instance, at a 0.5C discharge, the maximum energy delivered by 14s1p-‖ is 4104.5 Wh, and the minimum energy is 4021.7 Wh. However, at the same discharge rate, the maximum energy delivered by 14s9p-X| is only 3859 Wh, and the minimum energy is only 3718.8 Wh. The difference between the maximum and minimum is 82.8 Wh for 14s1p-‖ and 140.2 Wh for 14s9p-X|, i.e. 2.06% and 3.77% variation in the output energy, respectively.

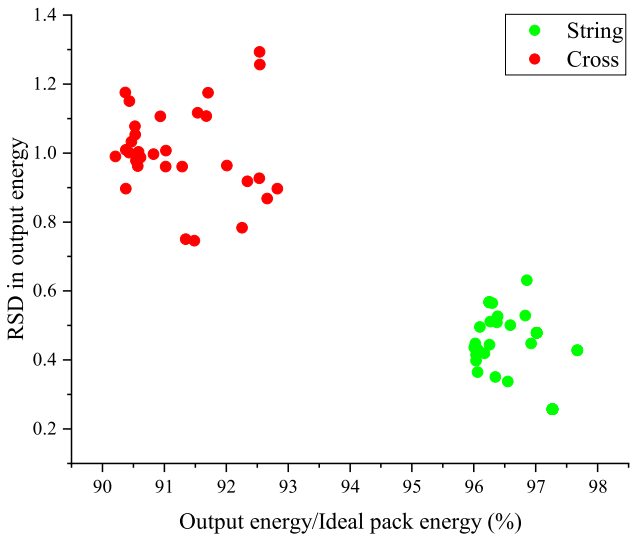

Fig. 9. Comparison of the ratio of mean output energy and ideal pack energy of each of the 74 pack configurations with the RSD (relative SD) in output energy of the same model.

Table 3
Best and worst pack configurations as mentioned in Fig. 14. Here σ denotes the usage standard deviation calculated from the work of Xie et al. [6], in simulating the discharge of pack configurations. Whereas 2σ denotes the usage of double these standard deviations.

Pack	14s9p	14s18p	21s24p
Best model at σ	14s1p-||	14s1p-||	7s1p-||
Worst model at σ	7s3p-X|	14s9p-X|	21s12p-X|
Best model at 2σ	14s1p-||	14s1p-||	7s1p-||
Worst model at 2σ	7s3p-X|	14s9p-X|	21s12p-X|

Similarly, on repeating the same analysis on the smaller 2.5 kWh pack, the pack 7s3p-XX has maximum and minimum energy output as 1983 Wh and 1862.8 Wh, which meant a variation of 120.2 Wh in the 20 instances of the same pack. This is a variation of 6.45% in energy.

For 14s18p pack, the mean energy delivered by each pack model was compared, Fig. 11(a) shows a line plot of all the various pack configurations for this. Many string-connected configurations, such as 14s1p-‖ and 14s6p-‖, deliver the maximum energy and overlap each other, while the cross-connected modules result in the lowest energy output. At a 0.5C discharge, 14s6p-‖ delivers 4068.3 Wh, while the 14s9p-X| only manages about 3780 Wh. Hence, the difference between the best and the worst configuration is 288.3 Wh at a 0.5C discharge. As we move to the right end of the plot, at 2.5C discharge, 14s1p-‖ delivers 3300 Wh, and 14s9p-X| provides an output of 3098.75 Wh. The difference amounts to 201.25 Wh. As the C-rate increases the difference in the energy output of the 14s1p-‖ and the 14s9p-X| packs decreases as shown in Fig. 11(b). Fig. 12(a) shows the relative SD in the energy output of different configurations. Fig. 12(b) shows the percentage of how other configurations compare with the best configuration in terms of delivered energy (Wh), at 1C discharge rate. Here, the output of 14s9p-X| is less than 7.09% of what the 14s1p-‖ has delivered. Some zero-value bars are present at the left end, indicating that they all delivered the same output energy.

We simulated 20 instances of the 14s1p module used in the 5 kWh pack at each multiplier and C rate. Here, the multiplier is a factor by which both the SD values i.e. voltage SD and capacity SD, are multiplied, simultaneously. This is done to study the pack performance as the variations in cell-to-cell parameters increase. The x-axis shows the variation in the multiplier. The SD values calculated from the work of Xie et al. [6] are 0.0315 for rated capacity and 0.0156 for nominal

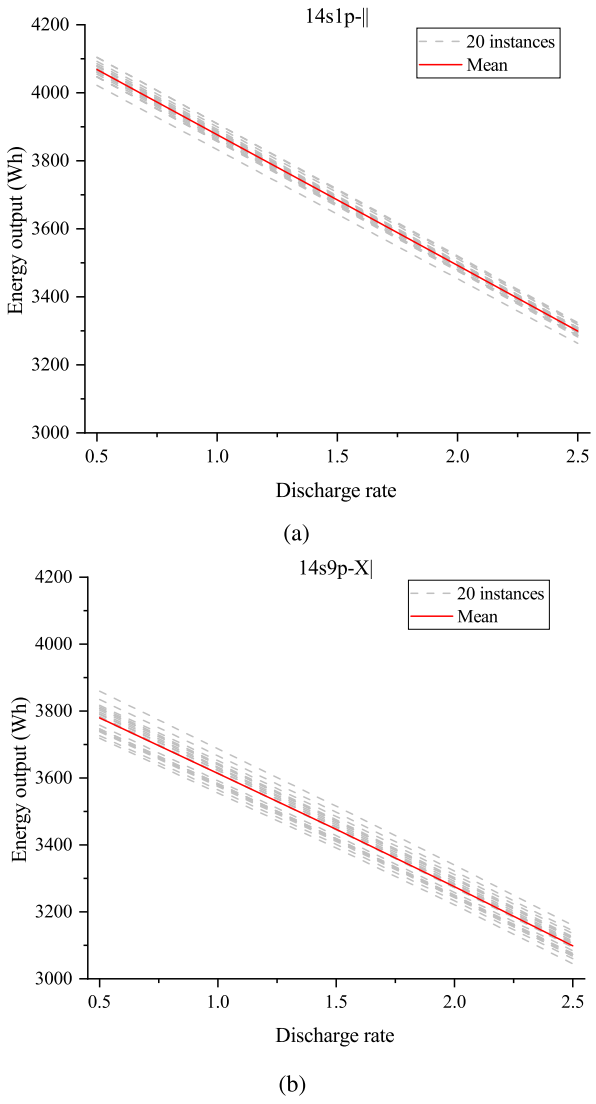

Fig. 10. Simulations are only done at the 5 discharge rates shown on the x-axis; the lines drawn show the expected energy output at all the other discharge rates. (a) Variations over 20 instances of a 14s1p-‖ connected 14s18p (5 kWh) pack. (b) Variations over 20 instances of a 14s9p-X| connected 14s18p pack.

voltage. As the multiplier increases, the SD in both the nominal voltage and the rated capacity increases.

Fig. 13 displays the variation of pack energy output with an increase in SD of cell parameters. Examining the 0.5C discharge data, the maximum and minimum energy delivered is the same, when the multiplier is zero, i.e., the SD in cell parameters is zero. The mean value of energy delivered here is 4192.6 Wh. When the multiplier is 3, the maximum, minimum, and difference in the energy delivered are 3891.4 Wh, 3729.2 Wh, and 162.2 Wh, respectively. Here, the mean and SD in the output energy of 20 instances is 3826 Wh and 52 Wh, respectively.

We compared the mean values of the energy output of all the extreme pack configurations cases for each pack size to the ideal pack energy of the pack in Fig. 14. The best and worst configurations of all three pack sizes are mentioned in Table 3. For a 14s18p pack, the 14s1p-‖ module delivers 2.98% less energy compared to the ideal pack energy. However, the 14s9p-X| module with cross connections delivers a higher reduction of 9.56% in energy. If the standard deviations in cell parameters are doubled, the 14s18p pack with the 14s1p-‖ module delivers 5.23% less energy, while the 14s9p-X| module for the same pack delivers the highest reduction of 18.28% in energy compared to the ideal pack.

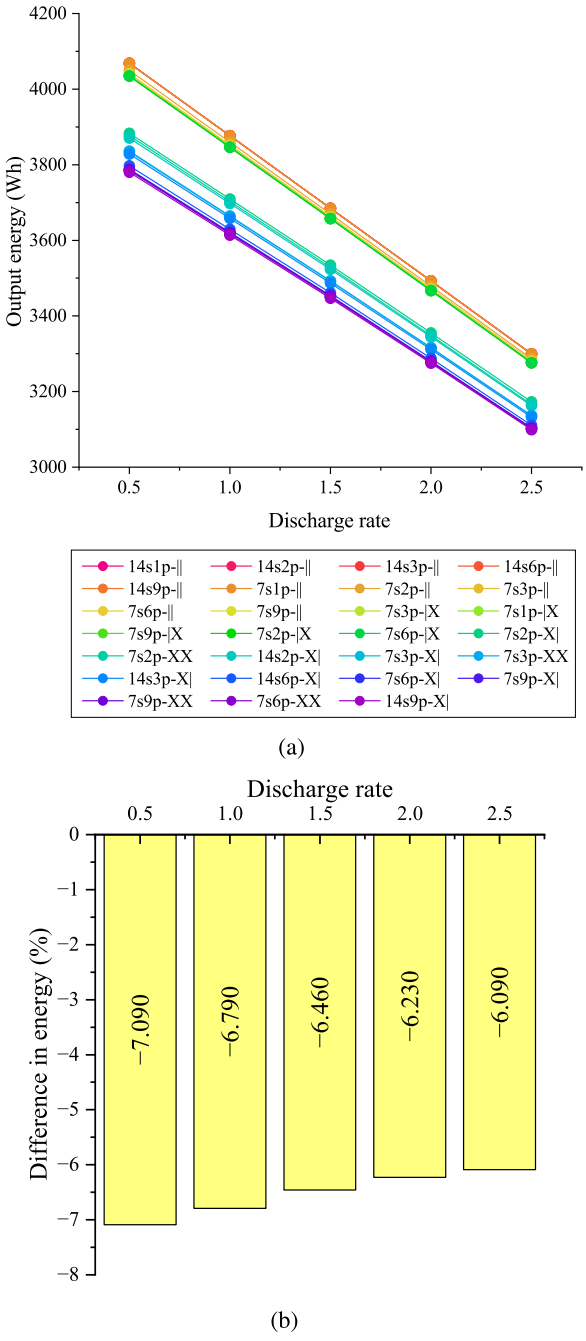

Fig. 11. Simulations are only done at the 5 discharge rates shown on the x-axis; the lines drawn show the expected energy output at all the other discharge rates. (a) Energy output of the 27 pack configurations of 14s18p pack. Every data point is a mean of 20 instances of that pack configuration at one of the five C rates. (b) Figure illustrates the difference between the best (14s1p-||) and the worst (14s9p-X|) pack configurations in energy output (%).

The internal behaviour of cells was studied during all the simulations mentioned above. Fig. 15 shows the average SDs in SoCs of cells of all the pack configurations of the 14s18p pack. The string cell connections like the 14s1p-|| module show an average SD in SoC of 0.459. On the other hand, this variation goes up to 1.27 for the 7s9p-XX module.

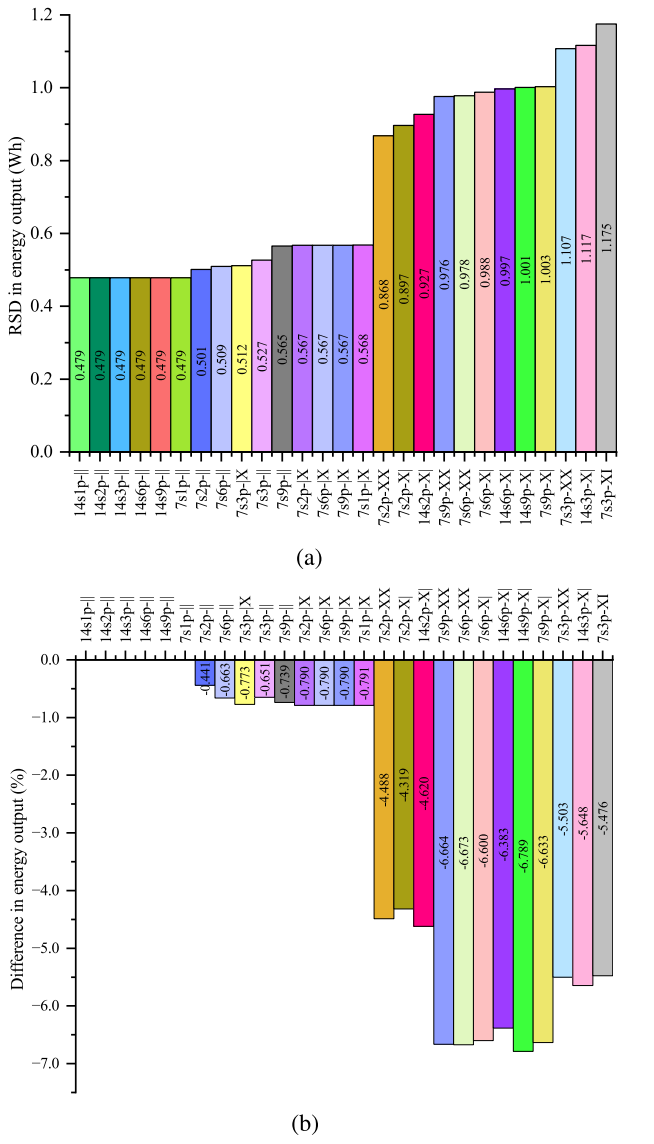

Fig. 12. (a) RSD (relative SD) between all the connection topologies for 14s18p pack, at 1C discharge rate. (b) Comparison of the decrement in output energy of each pack connection compared to the best pack connection i.e. 14s1p-||, at constant 1C discharge. To enable easier comparison between figures, the sorting order and the colours of models shown here is preserved for further figures showing all the models of the 14s18p pack. (For interpretation of the references to colour in this figure legend, the reader is referred to the web version of this article.)

3.2. Comparison at drive cycle discharge

The origins of the data used for simulating these drive cycle simulation has already been explained in the Design of Experiments Section 2.3.

Fig. 16(b) shows the mean energy that the battery packs discharged while being driven on drive cycles. For this part, we simulate the application of the considered battery packs in e-2Ws [49].

For instance, in the Zirakpur drive cycle, the best module is 14s1p-|| which delivered around 4119.8 Wh of energy, whereas the bottom most module 7s6p-XX, with both internal and external cross connections, is delivering 3857.36 Wh, which is 262.44 Wh difference in the energy. Looking at the distance, the 14s1p-|| equipped e-2W travelled 104.6 km and a 7s6p-XX e-2W travelled 97.9 km. Hence, a 262.44 Wh difference between the two pack configurations translated into an extra 6.74 km being driven by the superior 14s1p-|| equipped e-2 W, as seen from

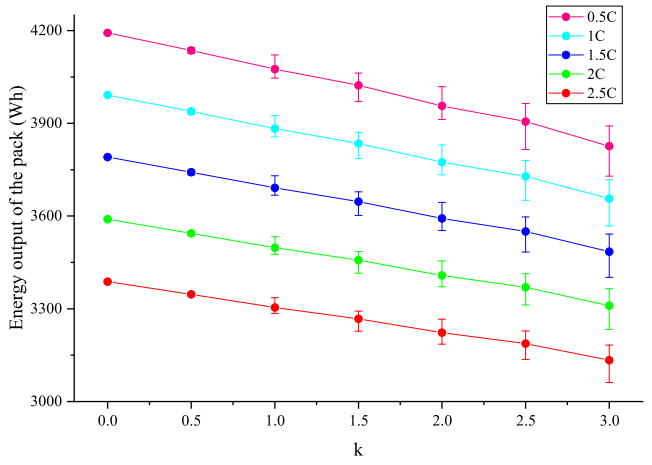

Fig. 13. Correlation between increasing SD in cell parameters and output Wh. 14s1p module with a 14s18p pack is used. 20 simulations have been performed at each C rate, cell parameters SD pair. SD in cells = k * SDs from [6] (Here k is the multiplier, which is displayed on the x-axis). The whiskers extending upwards and downwards from each point indicate the maximum and minimum values observed in 20 instances of pack simulations.

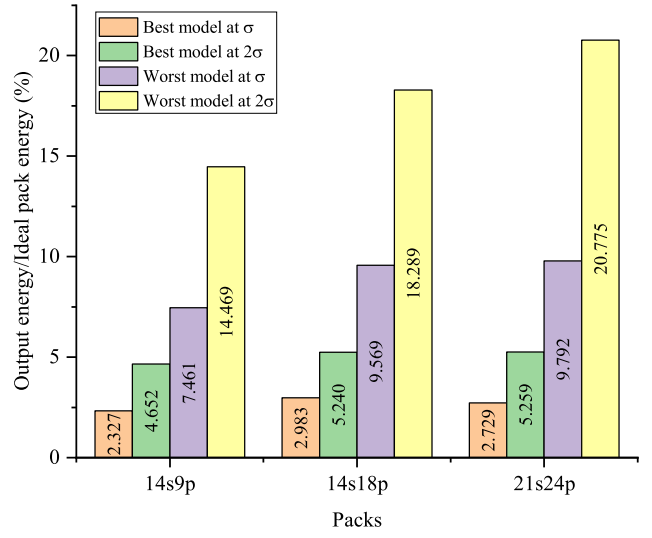

Fig. 14. Difference in energy delivered by the best and worst battery model within each pack size, compared to the ideal pack energy of the respective pack. This comparison is carried out at 1C discharge and for the original SDs in cell parameters, which is denoted by σ in the legend and for the double of it, denoted by 2σ.

Fig. 16, is around a 6.88% increase in the driving range between the best and the worst ways the cells can be connected inside the battery pack. For the same drive cycle but with the smaller 2.5 kWh pack, the best and the worst topologies had a difference of 100.73 Wh, which translated into a 2.52 km difference in the distance travelled by the e-2 W, a 5.25% increase in range. Similarly, for the 10 kWh equipped e-2 W, the best and the worst topologies had a difference of 571.53 Wh, which translated into a 14.6 km difference in the distance travelled by the e-2 W, a 7.33% increase in range. These were the mean values of the 20 instances of each pack topology described. Analysing the variations within the 20 instances, continuing with the Zirakpur drive cycle, the 14s1p equipped e-2W had a difference of 66.56 Wh between the maximum and the minimum energy delivered by the pack, this translated into a 1.72 km variation in range. Meanwhile, the 7s6p-XX e-2W had a variation of 148.4 Wh, which show a 3.86 km variation in the driving range. The corresponding figures for both the largest and the smallest pack are available in the section 1 of the supplementary.

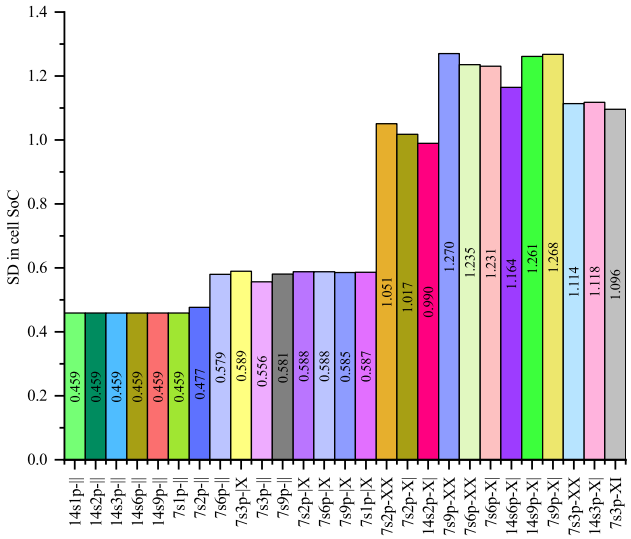

Fig. 15. The mean of SDs in SoC of each cell, in each pack configuration of the pack 14s18p, after 1000 s of discharge. All cells have the same initial SoC.

Table 4
Data of two parameters, at five different C rates, for two different types of connections, to estimate the pack performance parameters of a new pack size.

Connections	C_{Rate}	$\mu_{\mathrm{Wh}(cluster)}$	$\sigma_{R(cluster)}$
String	0.5	96.66	0.44
String	1	96.68	0.43
String	1.5	96.73	0.42
String	2	96.70	0.41
String	2.5	96.73	0.41
Cross	0.5	90.95	1.04
Cross	1	91.22	1.00
Cross	1.5	91.53	0.97
Cross	2	91.68	0.95
Cross	2.5	91.82	0.95

The correlation coefficient between the kinetic intensity of all of the drive cycles and the distance travelled is −0.347.

4. Empirical modelling

The performance of all 74 different configurations, comprising all three packs, simultaneously, for a specific C rate is studied in this section. The energy delivered by each configuration is compared to its respective ideal pack energy. This is compared with the relative SD in the energy output of each configuration.

The resulting plot is presented in Fig. 9. The points are clustered into two groups, one associated with string-connected modules and the other with cross-connected ones. The two mean points of these clusters were used to propose a relationship capable of computing the mean Wh and SD in the energy output of a new pack size. Consequently, simulations of smaller battery packs can be utilised to estimate the output performance of a larger battery pack.

After choosing a connection type i.e. cross or string, the corresponding cluster is to be selected and the following calculations need to be performed, or that cluster, to estimate new pack output energy and the SD in it. The $\mu_{\mathrm{Wh}(cluster)}$ and $\sigma_{R(cluster)}$ are already calculated from our data and are available in Table 4.

$$\mu_{\mathrm{Wh}(old)} = Mean\ of\ 20\ pack\ output\ \mathrm{Wh}\ for\ a\ model$$

$$\mu_{\mathrm{Wh}} = Expected\ \mathrm{Wh}\ output\ of\ the\ new\ pack$$

$$\mu_{\%\mathrm{Wh}(old)} = Mean\ \mathrm{Wh}\ (\%)\ of\ a\ cluster\ (x\text{-}axis)$$

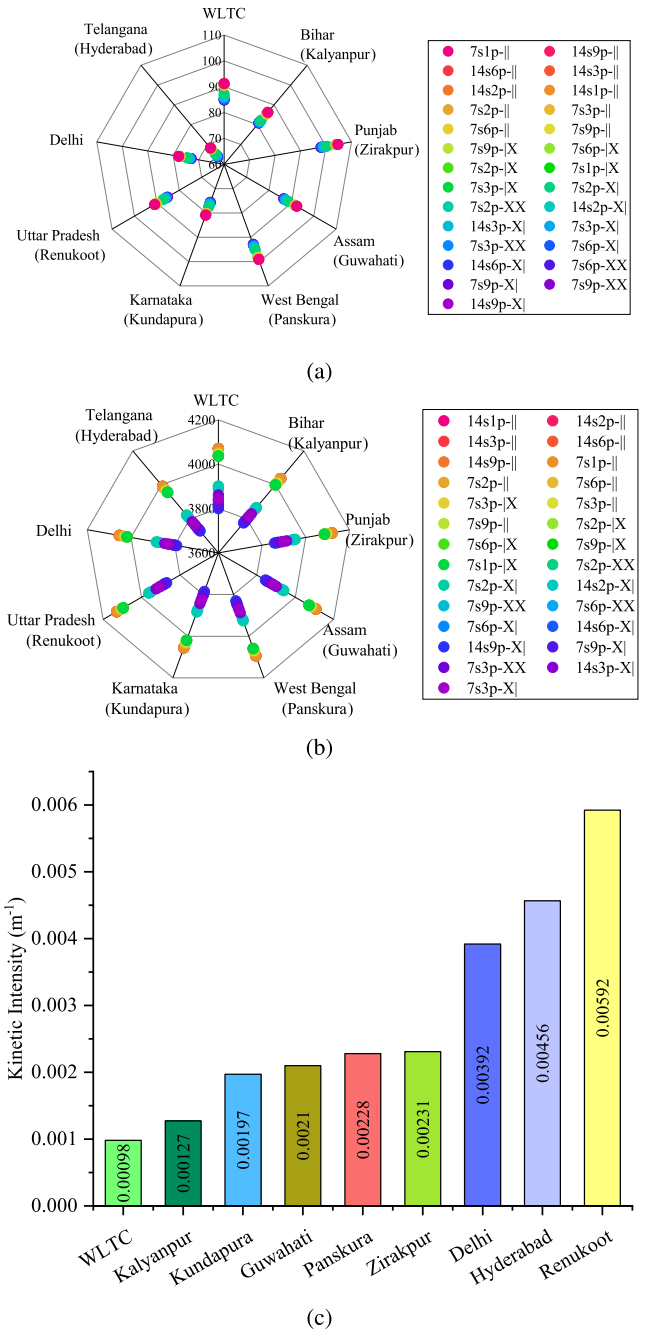

Fig. 16. It is assumed that the battery pack (14s18p) is installed inside an e-2 W, which is driven on nine different drive cycles. All the 27 pack models of 14s18p were evaluated. (a) Distance travelled by the e-2W (in km) for each drive cycle. (b) Energy delivered by the battery pack (in Wh) for each drive cycle. (c) Kinetic Intensity of each drive cycle.

$\mu_{\mathrm{Wh}(cluster)} = Mean\ of\ all\ \mu_{\%\mathrm{Wh}(old)}\ in\ a\ cluster$

$\sigma_{\mathrm{Wh}(old)} = SD\ in\ 20\ pack\ output\ \mathrm{Wh}\ for\ a\ model$

$\sigma_{\mathrm{Wh}} = Expected\ SD\ in\ output\ \mathrm{Wh}\ of\ the\ new\ pack$

$\sigma_{R(old)} = Relative\ SD\ in\ pack\ output\ energy\ (y\text{-}axis)$

$\sigma_{R(cluster)} = Mean\ of\ all\ \sigma_{R(old)}\ in\ a\ cluster$

$\mathrm{Wh}_{cell} = \mathrm{Wh}\ rating\ of\ the\ cell$

$DOD_{cell} = Depth\ of\ discharge\ of\ cell$

$N = Total\ cells\ in\ the\ new\ pack$

$N_{old} = Total\ cells\ in\ the\ new\ pack$

$n = Number\ of\ models\ in\ the\ cluster$

$$\mu_{\%\mathrm{Wh}(old)} = \frac{\mu_{\mathrm{Wh}} \times 100}{\mathrm{Wh}_{cell} \times N_{old}} \tag{1}$$

$$\sigma_{R(old)} = \frac{\sigma_{\mathrm{Wh}(old)} \times 100}{\mu_{\mathrm{Wh}(old)}} \tag{2}$$

$$\mu_{\mathrm{Wh}(cluster)} = \sum_{i=1}^{n} \frac{\mu_{\%\mathrm{Wh}(old)_i}}{n} \tag{3}$$

$$\sigma_{R(cluster)} = \sum_{i=1}^{n} \frac{\sigma_{R(old)_i}}{n} \tag{4}$$

$$\mu_{\mathrm{Wh}} = \frac{N \times \mathrm{Wh}_{cell} \times \mu_{\mathrm{Wh}(cluster)}}{100} \tag{5}$$

$$\sigma_{\mathrm{Wh}} = \frac{\mu_{\mathrm{Wh}} \times \sigma_{R(cluster)}}{100} \tag{6}$$

5. Assumptions and limitations

For the ease of simulating and studying the pack behaviour of so many different pack models, some assumptions were made along the way, which are listed below.

- Normal distribution is assumed for the variation of nominal cell capacity and voltage. The mean value is taken from the rated parameters provided by the manufacturer, while the SD is taken from the work of Xie et al. [6]. As the nominal parameters are real-valued random numbers. Hence, the distribution according to the central limit theorem turns out to be a Normal Distribution.
- Cells are distributed inside the battery pack randomly. Individual cell parameters cannot be measured on an assembly line. Hence, no order can be seen in cell distribution.
- Throughout the simulation, it is assumed that the developed model is temperature-independent. At the time of manufacturing, capacity is declared at standard temperature and pressure conditions (STP). Hence, there is no need to consider the thermal model of the pack. (As we are not looking into the life cycle of the pack).
- Capacity fading and cell degradation are not considered in the proposed method. Capacity fading or cell degradation does not come into the picture for new cells. This work is to estimate the capacity of a new battery pack.
- This method assumes that the SoC of each cell will be known. While in reality, the SoC calculation results from many voltage and current measurements throughout the battery pack and using those values through complex mathematical models which can approximately calculate SoC. Still, this is a viable option to pursue in laboratories, and the results of this method can then be extrapolated for commercial usage.

6. Discussion

We probed the energy delivery dynamics of packs with cells connected in cross configurations, laying the groundwork for future investigations. Slight differences in cell parameters in a battery pack cause an uneven distribution of the load current among parallel cells or cell strings. Internal paths within the pack also allow cells to discharge into one another, generating circulating currents. Our hypothesis suggests that the cell SoC variations, as depicted in Fig. 15, could be the underlying cause of the reduced output energy in cross-connected battery packs. These variations likely stem from the uneven distribution of current within cross-connected cells, a phenomenon also evident in previous studies [8,24]. It is possible that the elevated number of interconnections in cross-connected packs contributes to this uneven current distribution.

The difference between the energy output of a pack's best and worst configurations decreases as the discharge rate rises. This may be due to the higher C-rates discharging the pack so quickly that the variations in the cell do not get enough time to impact the energy output. Higher SDs in cell parameters lead to increased SDs in the pack output energy. The percentage Wh vs. SD plot, Fig. 9, displays two distinct clusters of points, one for all cross-connected configurations and another for string configurations. The string cluster shows lower SDs and higher output energy, whereas the cross-connected packs cluster has higher SDs and low energy output.

Fig. 12(a) shows that the SD in string-connected modules is lower compared to the cross-connected ones. Fig. 11(a) demonstrates the fact that string topology modules deliver more output energy compared to cross-connected ones. On average, the string topology delivered more than 7% the energy of the cross topology. Hence, string modules are better, both in terms of mean output energy delivered to the load and the variations of output energy from the mean.

As the SD in cell parameters increases, the output energy of the pack falls, and the SD in the output energy increases. Hence, it is necessary to keep the SD in cell parameters to a minimum.

The output energy from a pack decreases as the number of cross-connections between the cells increases, as seen in Fig. 14. A significant difference between the best and the worst topologies is evident. Essentially, a significant dip in output energy is observed compared to the ideal pack energy. Moreover, it is evident that doubling the SD in cell parameters implies about double the amount of decrement in output energy for each module and each pack, i.e., the percentage of decrease in output energy is highly proportional to the SD in cell parameters.

Essentially, the string-connected packs show the least average SD in cell SOCs, while the cross-connected ones show the highest average cell SoC SDs after discharging. This could be the reason why the cross-connected packs have performed so poorly compared to the string modules throughout the analysis. With lesser variations in the SoCs of cells, it can also be said that string-connected packs have a sort of SoC balancing effect on their cells compared to the cross-connected ones. Moreover, the cross-connected packs have many more internal paths allowing a chance of more circulating currents between cells. Additionally, as the cells alongside each other are a bit different, they share load currents unequally. Altogether, the weakest cell, with the least energy, discharges to the lower SOC limit first, triggering the pack cut-off from the load. This limits the amount of energy that the cross-connected packs can deliver compared to the string-connected ones.

A similar trend, as observed in the case of constant discharge rate, can be seen with the drive cycle discharge, i.e. the energy delivered and the distance driven by the vehicles with different pack topologies are different. Again, it was the string configuration of the pack that delivered the most range, and this range decreased with the increase in the cross-connections between the packs. Furthermore, the SD in the energy delivered increases as we move from the string to the cross-connected pack configurations.

We observed a loose correlation between the kinetic intensity of the drive cycles and the distance travelled by the vehicle. The obtained correlation coefficient is also negative, implying that the distance driven decreases with an increase in the kinetic intensity of the drive cycle.

An empirical model has been proposed using the data of all the topologies analysed in this work. This will help in getting a quick estimate of the output performance of a larger battery pack from the data accumulated by simulating various cross and string-connected models of smaller packs. This will reduce the computation time during the pack design process. Moreover, the proposed model can help in deciding the kind of configuration and cell-to-cell connections within a battery pack that will provide the maximum extractable energy during the design and manufacturing stage itself.

Lastly, the key findings from this work have been highlighted here in three major points: (I) The study revealed that series-connected packs exhibited higher energy output, which translated into a greater range for EVs compared to cross-connected battery packs. (II) As the standard deviation in cell capacity and voltage increased, the mean energy delivered by the pack decreased while the standard deviation in the energy increased. This reduction in mean energy was particularly pronounced in cross-connected pack configurations. (III) The higher variability in state-of-charge (SoC) among cells in cross-connected configurations was identified as the main contributor to this energy variation.

In summary, our research work contributes to the broader understanding of the impact of cell-to-cell parameter variation and pack configuration on energy and range variability, paving the way for continued advancements in designing optimal battery packs. By examining the contributing factors and proposing innovative strategies to mitigate these differences during pack design, this research work may mark a significant step forward in the search for sustainable transportation solutions.

7. Conclusion

The impact of cell-to-cell variations and pack connection topology has been investigated on the battery pack's performance. The study involved analysing three distinct pack sizes, resulting in a comprehensive assessment of 74 unique pack configurations. These configurations encompassed diverse combinations of both cell-to-cell and module-to-module connections, primarily classified as string and cross-connections. These various models were subjected to simulations across a range of constant C discharge rates and nine distinct drive cycles representative of driving conditions across different regions of India.

Additionally, an empirical model is proposed based on comprehensive simulation data. This model offers a means to estimate the average energy and standard deviation in energy delivery at various C rates for battery packs composed of identical cells but differing dimensions. Similarly, this methodology can be adapted to different cell chemistries by updating the constants specific to the particular chemistry used.

CRediT authorship contribution statement

Sourabh Singh: Writing – review & editing, Writing – original draft, Visualization, Methodology, Investigation, Formal analysis, Data curation, Conceptualization. **Sarbani Mandal:** Writing – review & editing, Writing – original draft, Visualization, Methodology, Investigation, Formal analysis, Data curation, Conceptualization. **Sai Krishna Mulpuri:** Writing – review & editing, Visualization, Software, Investigation, Formal analysis. **Bikash Sah:** Writing – review & editing, Writing – original draft, Visualization, Validation, Supervision, Software, Project administration, Methodology, Investigation, Formal analysis, Conceptualization. **Praveen Kumar:** Writing – review & editing, Supervision, Formal analysis, Conceptualization.

Declaration of competing interest

The authors declare that they have no known competing financial interests or personal relationships that could have appeared to influence the work reported in this paper.

Data availability

Data will be made available on request.

Acknowledgments

The publication cost is partially covered by the Library Hochschule Bonn-Rhein-Sieg and the Startförderung (28731207) granted to the corresponding author from Hochschule Bonn-Rhein-Sieg.

Appendix A. Supplementary data

Supplementary material related to this article can be found online at https://doi.org/10.1016/j.etran.2024.100329.

References

[1] Mukherjee A. Global electric vehicle sales crossed 10 million in 2022, Q4 sales up 53% YoY. 2023, URL: https://www.counterpointresearch.com/global-ev-sales-Q4-2022.
[2] Dalvi A. EV sales in India in 2022 record 210% growth, cross a million for the first time. 2022, URL: https://bit.ly/3XugJ0K.
[3] Ellson A. Electric car ranges '20% lower than advertised'. 2023, URL: https://www.thetimes.co.uk/article/electric-car-ranges-20-lower-than-advertised-8dptvjn39?shareToken=d9e500f1f5c61356fd593b501620fec0.
[4] Mruzek M, Gajdac I, Kucera L, Barta D. Analysis of parameters influencing electric vehicle range. Procedia Eng 2016;134:165–74.
[5] Chen J, Zhou Z, Zhou Z, Wang X, Liaw B. Impact of battery cell imbalance on electric vehicle range. Green Energy Intell Transp 2022;1(3):100025.
[6] Xie L, Ren D, Wang L, Chen Z, Tian G, Amine K, He X. A facile approach to high precision detection of Cell-to-Cell variation for li-ion batteries. Sci Rep 2020;10(1):7182.
[7] Dubarry M, Vuillaume N, Liaw BY. Origins and accommodation of cell variations in Li-ion battery pack modeling. Int J Energy Res 2010;34(2):216–31.
[8] Liu X, Ai W, Naylor Marlow M, Patel Y, Wu B. The effect of cell-to-cell variations and thermal gradients on the performance and degradation of lithium-ion battery packs. Appl Energy 2019;248:489–99.
[9] Reiter A, Lehner S, Bohlen O, Sauer DU. Electrical cell-to-cell variations within large-scale battery systems - A novel characterization and modeling approach. J Energy Storage 2023;57:106152.
[10] Schindler M, Sturm J, Ludwig S, Schmitt J, Jossen A. Evolution of initial cell-to-cell variations during a three-year production cycle. eTransportation 2021;8:100102.
[11] An F, Zhang W, Sun B, Jiang J, Fan X. A novel battery pack inconsistency model and influence degree analysis of inconsistency on output energy. Energy 2023;271:127032.
[12] Chang L, Ma C, Zhang C, Duan B, Cui N, Li C. Correlations of lithium-ion battery parameter variations and connected configurations on pack statistics. Appl Energy 2023;329:120275.
[13] Yang C, Wang X, Fang Q, Dai H, Cao Y, Wei X. An online SOC and capacity estimation method for aged lithium-ion battery pack considering cell inconsistency. J Energy Storage 2020;29:101250.
[14] Ziegler A, Oeser D, Hein T, Montesinos-Miracle D, Ackva A. Reducing cell to cell variation of lithium-ion battery packs during operation. IEEE Access 2021;9:24994–5001.
[15] Miyatake S, Susuki Y, Hikihara T, Itoh S, Tanaka K. Discharge characteristics of multicell lithium-ion battery with nonuniform cells. J Power Sources 2013;241:736–43.
[16] Zhou L, Zheng Y, Ouyang M, Lu L. A simulation study on parameter variation effects in battery packs for electric vehicles. Energy Procedia 2017;105:4470–5, 8th International Conference on Applied Energy, ICAE2016, 8-11 October 2016, Beijing, China.
[17] Dubarry M, Pastor-Fernández C, Baure G, Yu TF, Widanage WD, Marco J. Battery energy storage system modeling: Investigation of intrinsic cell-to-cell variations. J Energy Storage 2019;23:19–28.
[18] Duan B, Li Z, Gu P, Zhou Z, Zhang C. Evaluation of battery inconsistency based on information entropy. J Energy Storage 2018;16:160–6.
[19] Fan X, Zhang W, Sun B, Zhang J, He X. Battery pack consistency modeling based on generative adversarial networks. Energy 2022;239:122419.
[20] Luan C, Ma C, Wang C, Chang L, Xiao L, Yu Z, Li H. Influence of the connection topology on the performance of lithium-ion battery pack under cell-to-cell parameters variations. J Energy Storage 2021;41:102896.
[21] Birrell SA, McGordon A, Jennings PA. Defining the accuracy of real-world range estimations of an electric vehicle. In: 17th international IEEE conference on intelligent transportation systems. ITSC, 2014, p. 2590–5.
[22] Chang L, Zhang C, Wang T, Yu Z, Cui N, Duan B, Wang C. Correlations of cell-to-cell parameter variations on current and state-of-charge distributions within parallel-connected lithium-ion cells. J Power Sources 2019;437:226869.
[23] Schindler M, Sturm J, Ludwig S, Schmitt J, Jossen A. Evolution of initial cell-to-cell variations during a three-year production cycle. eTransportation 2021;8:100102.
[24] Rumpf K, Rheinfeld A, Schindler M, Keil J, Schua T, Jossen A. Influence of cell-to-cell variations on the inhomogeneity of lithium-ion battery modules. J Electrochem Soc 2018;165(11):A2587.
[25] Song Z, Yang N, Lin X, Pinto Delgado F, Hofmann H, Sun J. Progression of cell-to-cell variation within battery modules under different cooling structures. Appl Energy 2022;312:118836.
[26] Wildfeuer L, Lienkamp M. Quantifiability of inherent cell-to-cell variations of commercial lithium-ion batteries. eTransportation 2021;9:100129.
[27] Zilberman I, Ludwig S, Jossen A. Cell-to-cell variation of calendar aging and reversible self-discharge in 18650 nickel-rich, silicon–graphite lithium-ion cells. J Energy Storage 2019;26:100900.
[28] Rumpf K, Naumann M, Jossen A. Experimental investigation of parametric cell-to-cell variation and correlation based on 1100 commercial lithium-ion cells. J Energy Storage 2017;14:224–43.
[29] Beck D, Dechent P, Junker M, Sauer DU, Dubarry M. Inhomogeneities and cell-to-cell variations in lithium-ion batteries, a review. Energies 2021;14(11).
[30] Lee D, Kang S, Shin CB. Modeling the effect of cell variation on the performance of a lithium-ion battery module. Energies 2022;15(21).
[31] Ganesan N, Basu S, Hariharan KS, Kolake SM, Song T, Yeo T, Sohn DK, Doo S. Physics based modeling of a series parallel battery pack for asymmetry analysis, predictive control and life extension. J Power Sources 2016;322:57–67.
[32] Baumhöfer T, Brühl M, Rothgang S, Sauer DU. Production caused variation in capacity aging trend and correlation to initial cell performance. J Power Sources 2014;247:332–8.
[33] Santhanagopalan S, White R. Quantifying cell-to-cell variations in lithium ion batteries. Int J Electrochem 2012;2012.
[34] Schuster SF, Brand MJ, Berg P, Gleissenberger M, Jossen A. Lithium-ion cell-to-cell variation during battery electric vehicle operation. J Power Sources 2015;297:242–51.
[35] Devie A, Dubarry M. Durability and reliability of electric vehicle batteries under electric utility grid operations. Part 1: Cell-to-cell variations and preliminary testing. Batteries 2016;2(3).
[36] Dos Reis G, Strange C, Yadav M, Li S. Lithium-ion battery data and where to find it. Energy AI 2021;5:100081.
[37] Naaz F, Channegowda J. A probabilistic forecasting approach towards generation of synthetic battery parameters to resolve limited data challenges. Energy Storage 2022;4(4):e297.
[38] Naaz F, Herle A, Channegowda J, Raj A, Lakshminarayanan M. A generative adversarial network-based synthetic data augmentation technique for battery condition evaluation. Int J Energy Res 2021;45(13):19120–35.
[39] Qiu X, Wang S, Chen K. A conditional generative adversarial network-based synthetic data augmentation technique for battery state-of-charge estimation. Appl Soft Comput 2023;142:110281.
[40] Pyne M, Yurkovich BJ, Yurkovich S. Generation of synthetic battery data with capacity variation. In: 2019 IEEE conference on control technology and applications. CCTA, IEEE; 2019, p. 476–80.
[41] Goodfellow I, Pouget-Abadie J, Mirza M, Xu B, Warde-Farley D, Ozair S, Courville A, Bengio Y. Generative adversarial nets. Adv Neural Inf Process Syst 2014;27.
[42] Adiga S, Attia MA, Chang W-T, Tandon R. On the tradeoff between mode collapse and sample quality in generative adversarial networks. In: 2018 IEEE global conference on signal and information processing. GlobalSIP, IEEE; 2018, p. 1184–8.
[43] Zhang K. On mode collapse in generative adversarial networks. In: Artificial neural networks and machine learning–ICANN 2021: 30th international conference on artificial neural networks, bratislava, slovakia, September 14–17, 2021, proceedings, part II 30. Springer; 2021, p. 563–74.
[44] Mirza GIP-AJ. M Xu B Warde-Farley D Ozair S Courville A Bengio Y Generative adversarial networks. Commun Acm 2020;63(11):139.
[45] Barnett SA. Convergence problems with generative adversarial networks (gans), arXiv preprint arXiv:1806.11382.
[46] Kim R, Weon S. Product specification of LG INR21700 M50 18.20 Wh, rechargeable lithium ion battery. 2016, URL: https://www.dnkpower.com/wp-content/uploads/2019/02/LG-INR21700-M50-Datasheet.pdf.
[47] Chen C-H, Brosa Planella F, O'Regan K, Gastol D, Widanage W, Kendrick E. Development of experimental techniques for parameterization of multi-scale lithium-ion battery models. J Electrochem Soc 2020;167.

[48] Nyman A, Behm M, Lindbergh G. Electrochemical characterisation and modelling of the mass transport phenomena in LiPF6–EC–EMC electrolyte. Electrochim Acta 2008;53(22):6356–65.

[49] Kumar P, Singh OJ, Mulpuri SK, Sah B. Electric 2-wheeler drive cycle based drivetrain sizing : A comprehensive analysis. 2020, URL: https://www.iitg.ac.in/e_mobility/drivetrain_sizing_report.pdf.

[50] Catenaro E, Onori S. Experimental data of lithium-ion batteries under galvanostatic discharge tests at different rates and temperatures of operation. Data Brief 2021;35:106894.